Integrative Biology

REVIEW ARTICLE

View Article Online
View Journal | View Issue

Cite this: *Integr. Biol.*, 2016, **8**, 394

Received 8th October 2015,
Accepted 7th December 2015

DOI: 10.1039/c5ib00252d

www.rsc.org/ibiology

Build to understand: synthetic approaches to biology

Le-Zhi Wang,[a] Fuqing Wu,[b] Kevin Flores,[c] Ying-Cheng Lai[ade] and Xiao Wang*[b]

In this review we discuss how synthetic biology facilitates the task of investigating genetic circuits that are observed in naturally occurring biological systems. Specifically, we give examples where experimentation with synthetic gene circuits has been used to understand four fundamental mechanisms intrinsic to development and disease: multistability, stochastic gene expression, oscillations, and cell–cell communication. Within each area, we also discuss how mathematical modeling has been employed as an essential tool to guide the design of novel gene circuits and as a theoretical basis for exploring circuit topologies exhibiting robust behaviors in the presence of noise.

Insight, innovation, integration

Gene regulatory networks (GRNs) are central to the fundamental mechanisms regulating cell function and behavior. The presence of feedbacks and stochasticity can make the logic of GRNs non-intuitive. Small networks can be simulated in a "dry lab" setting, and also be engineered in a "wet lab" setting to probe detailed dynamics of an integrated set of genes. In this review we discuss how synthetic biology facilitates the task of investigating genetic circuits that are observed in naturally occurring biological systems. Specifically, we give examples where experimentation with synthetic gene circuits has been used to understand four fundamental mechanisms intrinsic to development and disease: multistability, stochastic gene expression, oscillations, and cell–cell communication.

1 Introduction

The rapid development of synthetic biology over the last 15 years has made it possible to engineer DNA sequences,[1–4] design genetic circuits,[5–7] synthesize genomes[8–10] and even reprogram cell fates.[11] This young and emerging field has shown great potential in various application areas, including bioenergy,[12–14] biopharmaceuticals,[15–18] bioremediation,[19–22] and regenerative medicine.[23–25] In addition to the development of enabling technologies with clinical and industrial applications, synthetic biology approaches have also proven to be very effective in studying fundamental operating principles of biology.[26–30]

Synthetic biology greatly simplifies the task of investigating genetic circuits that are ubiquitous in nature. In concert with mathematical modeling, the ability to synthesize genetic circuits greatly enhances our ability to test hypotheses about the underlying principles guiding developmental, disease, evolutionary, and adaptive cellular processes. Specifically, synthetic biology enables the possibility of studying commonly occurring gene regulatory network "motifs" or modules in isolation from larger networks that they might be embedded within. Once a network motif's function is understood and can be robustly engineered it can then be exploited to build novel cellular devices with clinical, therapeutic, or other biotechnology applications.

The use of mathematical modeling and analysis in synthetic biology enables the ability to systematically quantify functional attributes of commonly occurring gene network motifs and to discover novel motifs with useful functions. Modeling has been an essential tool for predicting the function of gene networks constructed from smaller motifs, since such networks may have complex topologies with multiple feedbacks that lead to nonlinear and non-intuitive dynamics. Moreover, stochastic models of genetic circuits have been useful for understanding how to engineer networks with dynamic behaviors that are robust in the presence of intracellular noise or variable environmental signalling. Once parameterized by experimental data, mathematical models can be used to run *in silico* experiments that are highly accurate at capturing the dynamics of wet lab experiments, thereby reducing the experimental cost of *de novo* gene circuit engineering.

[a] *School of Electrical, Computer and Energy Engineering, Arizona State University, Tempe, Arizona 85287, USA*
[b] *School of Biological and Health Systems Engineering, Arizona State University, Tempe, Arizona 85287, USA. E-mail: xiaowang@asu.edu*
[c] *Department of Mathematics, Center for Quantitative Sciences in Biomedicine, Center for Research in Scientific Computation, North Carolina State University, Raleigh, North Carolina 27695, USA*
[d] *Institute for Complex Systems and Mathematical Biology, King's College, University of Aberdeen, Aberdeen AB24 3UE, UK*
[e] *Department of Physics, Arizona State University, Tempe, Arizona 85287, USA*

Finally, experimentally verified mathematical reasoning makes it possible to develop theorem like dogmas for biology, just like it did for physics in the last century, which would greatly improve our understanding of life.

Here we review synthetic biology studies and mathematical methods used to support and guide experimental design. We frame our review by discussing four actively researched types of biological phenomena that arise in developmental and disease processes, and that have been explored using synthetic biology: multistability, stochastic gene expression, oscillations, and cell–cell communication.

2 Multistability

Multistability, the property of having multiple stable steady states in a dynamical system, has been proposed as a principle that guides cell differentiation and development in biological systems, with cellular states represented as either valleys in the developmental landscape[31,32] or as dynamic attractors in a high-dimensional gene expression space.[33–35] According to Waddington's epigenetic landscape theory,[31] cells are pictured as marbles that run downhill through a bifurcating valley and different routes lead to distinct cell phenotypes. Junctions in the landscape represent where cells may make a decision between steady states, based on the local dynamics of gene regulatory networks (GRNs) and external perturbations. GRNs regulate/control most of the important biological reactions, including metabolism, signal transduction, cell division and differentiation, and tissue development. However, it is often intractable to investigate the underlying principles of multistability and cell-fate decision in a natural setting. Synthetic biology provides an effective platform to decompose the

Le-Zhi Wang

Le-Zhi Wang is a PhD candidate in Electrical Engineering at Arizona State University, USA. She received her Bachelor of Science Degree from Donghua University, China. Her research areas include nonlinear dynamics, control of complex networks and gene regulation networks. Currently, she is working on building controllability framework for nonlinear dynamical networks and using network sciences approaches to reveal fundamental mechanisms in stem cell differentiation. She can be contacted by e-mail at Lezhi.Wang@asu.edu.

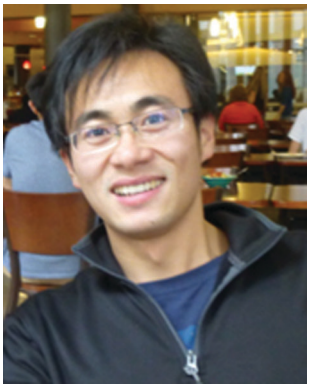

Fuqing Wu

Fuqing Wu is a PhD candidate in Biomedical Engineering at Arizona State University, USA. He received his Master Degree from the Wuhan Institute of Virology, Chinese Academy of Sciences. His research interests include synthetic gene circuit and molecular evolution. Particularly, he is interested in combining mathematical modeling with experimental validations to reveal the fundamental mechanisms generating multistability and state transition dynamics during stem cell differentiation. He can be contacted by e-mail at fuqingwu@asu.edu.

Kevin Flores

Dr Kevin Flores is an Assistant Professor in the Department of Mathematics and a member of the Center for Quantitative Sciences in Biomedicine and Center for Research in Scientific Computation at North Carolina State University. He received his PhD from Arizona State University in 2009, and had post-doctoral training for two years in Life Sciences at Arizona State University and three years in Applied Mathematics at North Carolina State University. His current research interests are in optimal experimental design, parameter estimation, and uncertainty quantification with applications to systems biology, precision medicine and environmental toxicology. He can be contacted by e-mail at kevinflores83@gmail.com.

Ying-Cheng Lai

Dr Ying-Cheng Lai is a Professor of Electrical Engineering and a Professor of Physics at Arizona State University, USA and the Sixth Century Chair in Electrical Engineering at the University of Aberdeen, UK. He received his PhD degree in Physics (Nonlinear Dynamics) from the University of Maryland at College Park in 1992 and had a two-year post-doctoral training in Biomedical Engineering at Johns Hopkins University School of Medicine. His current research interests are in nonlinear dynamics, complex networks, quantum transport, graphene physics, biological physics and signal processing. He can be contacted by e-mail at Ying-Cheng.Lai@asu.edu

complex networks into small regulatory motifs. These motifs can be further rationally designed and engineered using standardized genetic components to reveal underlying regulatory mechanisms.

The simplest example is one in which bistability enables cells to switch back and forth between two stable steady states. In general, bistability can arise from mutually inhibitory networks or positive-feedback loops.[36] A myriad of modeling and experimental studies have been performed to investigate the nonlinear dynamics and state transitions of bistable systems[5,37–40] and their applications, including the detection of chemical pollution through an engineered plant sensor,[41] creating photographs by controlling gene expression in *Escherichia coli* (*E. coli*),[42] and using *E. coli* strains to sense DNA damage.[43]

In 2000 Gardner *et al.*[5] paved the way for developing synthetic biology with their ground-breaking work on the "toggle switch" circuit. In this circuit, two repressible genes and their corresponding promoters were used to assemble a genetic toggle switch. For example, the authors used LacI–P_{LacI} and TetR–P_{Tet} combinations. The LacI protein could inhibit *TetR* transcription by binding the P_{LacI} promoter while TetR could bind P_{Tet} and block *LacI* transcription, forming a mutually inhibitory network. The strength of the two mutual inhibitions could be controlled by exogenous induction of isopropyl-D-1-thiogalactopyranoside (IPTG) and anhydrotetracycline (ATc) (Fig. 1a). Using mathematical modeling and experiments, it was verified that the toggle switch system could flip between two states with induction and display robust bistability.

This proof-of-concept design has also been implemented in mammalian cells[38] and yeast.[39] For example, the Fussenegger group[38] engineered a mammalian epigenetic transgene switch in which E-KRAB and PIP-KRAB expressed on two individual plasmids could inhibit each other by binding to *ETR* and *PIR* operators in their respective promoters. The induction of antibiotics indicated that this epigenetic circuitry exhibited two

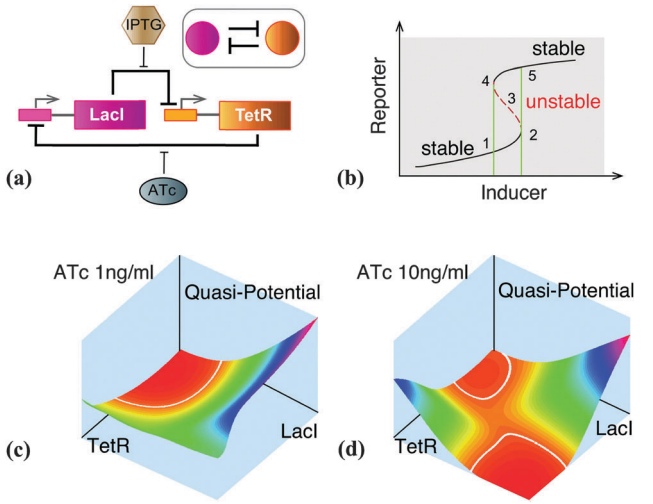

Fig. 1 Multistability in synthetic biology. (a) Schematic diagram of a typical toggle gene circuit based on Gardner *et al.* (2000).[5] In this circuit, two genes, *LacI* and *TetR*, mutually inhibit each other, which can be regulated by IPTG and ATc, respectively. The inset cartoon is a simplified diagram to demonstrate an abstract form of the network topology. (b) A bifurcation diagram can be used to find the inducer concentration range for bistability. Here, five points are marked to illustrate different stability regions. In the diagram, 1, 2, 4 and 5 are on the black solid lines and represent stable steady states; 3 is on the red dashed line and represents an unstable state. The system is bistable between 1 and 5, and monostable when the inducer concentration is below 1 and above 5. (c and d) Landscape of a bi-stable system under different concentrations of inducer (ATc). On each subfigure, white lines are circled stable steady states, which are used to locate attractor basins. It is shown that with different inducer concentrations, the system has a different landscape and steady states. In (c), the system has only one stable steady state; while in (d), the system is bistable. Based on Wu *et al.* (2013).[39]

stable expression states: high E-KRAB with low PIP-KRAB, and low E-KRAB with high PIP-KRAB. Furthermore, the bistable expression profiles were fully reversible even after rounds of expression switching. Interestingly, the system also showed long-term bistability in mice, suggesting that synthetic gene networks could be used as therapeutic devices in clinic in the future. Wu *et al.*[39] engineered synthetic gene networks to explore potential mechanisms for stochastic cell fate determination in yeast (*Saccharomyces cerevisiae*). Mutual inhibitory networks composed of two genes (*LacI* and *TetR*, Fig. 1a) were constructed using three different promoters and bistability was further investigated by experiments showing hysteresis (glossary: bifurcation diagram), which is an indicator of a bistable system. Primary experimental data were then used to calibrate parameters for a mathematical model of the LacI/TetR network. Ordinary differential equation (ODE) models (glossary: ODE) were built to simulate reactions influencing LacI and TetR expression. Parameters from the model were fit to experimental data of ATc dose response curves[44] and bistable regions were subsequently predicted using a numerical search with the parameterized model. In particular, a bifurcation diagram (glossary: bifurcation diagram) was used to find bistable regions for the LacI/TetR network for each of the three different strains and only a few parameters needed to be modified for different promoter strains (Fig. 1b).

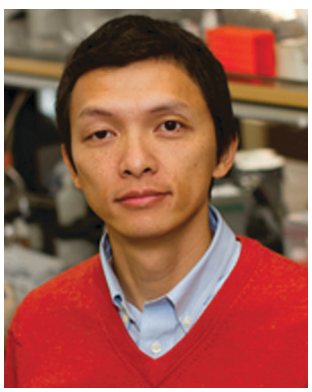

Xiao Wang

Dr Xiao Wang is an Assistant Professor in Biomedical Engineering at Arizona State University, USA. He received his PhD degree from the University of North Carolina at Chapel Hill in 2006. As the Principal Investigator of the Systems and Synthetic Biology Research Group, he is interested in using both forward (synthetic biology) and reverse (systems biology) engineering approaches to understand biology. Specific research topics include engineering synthetic multistable gene networks, systems biology research on small network motifs with feedbacks, understanding the role of noise in cell differentiation and development, and analysing molecular evolution. He can be contacted by e-mail at xiaowang@asu.edu

Then, quasi-potential energy landscapes (glossary: energy landscape) under different doses of ATc were visualized (Fig. 1c and d). The numerical results suggested that random outcomes of cell fate would be realized when the cell's initial state stayed on the boundary between the two attractors in a multistable landscape. To test this hypothesis experimentally, the authors linked the synthetic gene networks with the yeast cell's natural glucose–galactose metabolism to achieve the specific initial condition where no LacI or TetR are expressed in the cells. Cells from these experiments diverged into different final states. In summary, both theoretical and experimental analyses suggested that stochastic and irreversible cell fate determination could be realized by initializing cells at the attractors' basin boundaries.

Positive feedback is another ubiquitous topological structure found in nature that has the capacity to generate bistability. For example, the key regulatory mechanism for bacteria quorum-sensing systems is positive feedback motifs, which enable cells to make binary decisions in responding to environmental signals.[45] In eukaryotes, positive feedback loops embedded in gene networks regulate stem cell differentiation and development. For instance, positive feedback between the transcription factor *PU.1* and the cell cycle controls lymphoid and myeloid differentiation;[46] positive feedback between *Sox2* and *Sox6* in neural progenitor cells represses neuronal differentiation;[47] and Cdkn1c interacts with Myod to form a positive feedback that drives muscle differentiation.[48]

Robust bistable responses can also be achieved through coupling multiple positive feedback loops. Guided by theoretical model-based calculations, Chang *et al.*[49] tried to identify parameters controlling the size of a bistable range in order to build ultrasensitive systems. The authors created a composite system with two coherent positive feedback loops, where the promoter *glnK* drove expression of *glnG* and the *lacZYA* operon, respectively. The expression of glnG was simultaneously inhibited by the LacI protein and activated by the inducer IPTG. Functionally, glnG could auto-activate *glnK* transcription, forming a positive feedback, while the *LacY* gene product galactoside permease could facilitate cellular uptake of IPTG to promote glnG expression by deactivating LacI repression, forming another positive feedback. The experimental results showed that the double-positive feedback circuit exhibited potent bistability over a ~480-fold range of induction concentrations, whereas circuits with a single positive feedback showed a less than ~12-fold range. In the mathematical framework for bistability, the authors first focused on one single positive feedback and formulated mathematical terms that could result in an adjustment to the bistable range, including sensitivity of the production rate and the maximum difference of species concentrations. Then they studied the interaction of two feedback loops and found out that nonlinear rather than linear interactions would lead to bistability. In the analysis, the authors assumed that the production rate was determined by a feedback loop, degradation was linearly controlled by an external signal, and the steady state concentration of each species was state dependent. Together, this study provided a novel approach to improve the robustness and increase sensitivity of bistable systems for practical applications to control biological processes.

3 Gene expression stochasticity

Inherent stochasticity, or randomness, of the physical world has been widely recognized and well studied for a long time.[50–53] However, its significance in biological systems had not been appreciated until a group of pioneer synthetic biologists demonstrated its implication on population heterogeneity using elegantly designed synthetic gene circuits.[54–57] For example, Elowitz *et al.* led the way to analyze and quantify gene expression noise;[54] Ozbudak *et al.* used genetic parameters to regulate phenotypic variation;[55] Blake *et al.* discovered that noise contributes to heterogeneity in eukaryotic cell populations;[56] and Raser *et al.* identified mutations which could modify noise in eukaryotic gene expression.[57] Now stochasticity in gene expression is widely accepted as an important factor that may regulate a cell's fate,[58–61] adjust feedback loop behavior,[62–64] control cell size[65] and sense environmental fluctuations.[56,66]

Cellular decision-making is a widespread biological phenomenon across taxa, *e.g.*, lysis/lysogeny state transitions in bacteriophage lambda, the sporulation/competence decision system in *Bacillus subtilis*, and spontaneous differentiation into a specific subtype from embryonic stem cells in mammals.[67] The choice of cell fate is often driven by GRNs, extrinsic stimuli, and intrinsic stochastic fluctuations in gene expression (noise). Noise has multiple origins such as randomness in biochemical reactions including gene transcription and translation, fluctuations in signal transduction, and overall variability in cellular mRNA/protein degradation rates, cell size, and stage in the cell division process.[68,69] Although noise is usually thought to be detrimental to cell function and may even cause disease, it can also be advantageous for expression (phenotypic) diversity,[70,71] cell growth,[72,73] flexibility in cell adaptation,[59,74] and evolution.[75–77]

A key line of research has investigated the extent to which noise functions in the cell-fate decision making process. Experimental evidence indicates that that noise plays a critical role in the state choice of multistable systems. Taking the above "toggle switch" circuit[5] as an example of a bistable system, only one state was anticipated for the pTAK117 toggle in the presence of ~40 μM IPTG. Instead, the system exhibited a bimodal distribution, which has also been experimentally observed in other multistable systems, including the lactose operon system and synthetically engineered positive feedback systems.[43,78,79] The bimodal distribution of the 'toggle switch' circuit is very robust in yeast as Wu *et al.*[39] found out that inherent stochasticity in gene expression does not lead to state transitions. Moreover, the Dubnau group[80] demonstrated that noise in *comK* expression could be utilized to drive *Bacillus subtilis* cells to a competent state. Using an RNA FISH (fluorescence *in situ* hybridization) technique, they detected and counted the number of mRNA molecules from the coexpressed genes *comK* and *comK-M2* driven by the same *comK* promoter (Fig. 2a). The authors proposed a mathematical model based on a positive

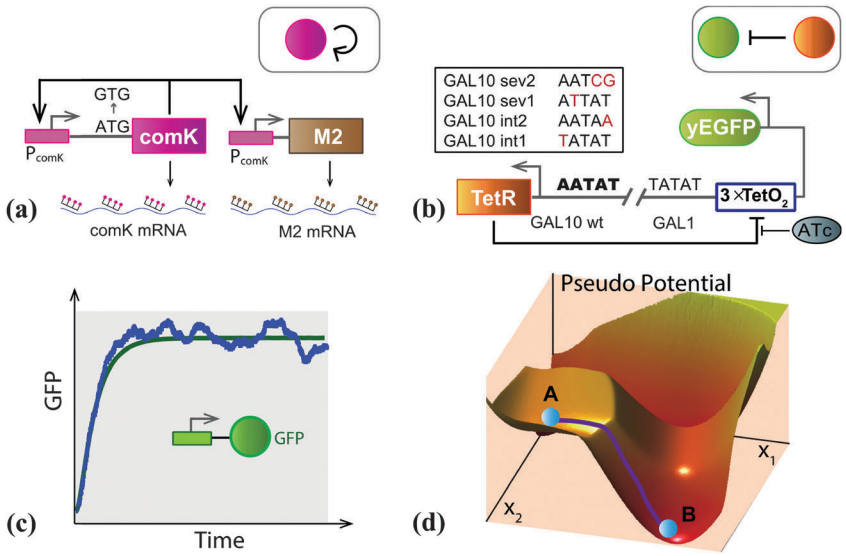

Fig. 2 Stochasticity in gene circuits. (a) Schematic diagram of regulation in *Bacillus subtilis* based on Maamar *et al.* (2007).[80] In this circuit, promoter P_{ComK} controls *comK* and *M2* expression, whose mRNAs could be recognized and bound by fluorescent probes. The inset cartoon illustrates the main part of the network in an abstract form. (b) Illustration of a noise control gene circuit in yeast (from Murphy *et al.* (2010)).[83] Five yeast strains including wild type and four TATA box mutations in the *GAL10* promoter were engineered to control gene expression noise levels. In this circuit, TetR driven by the *GAL10* promoter binds to $TetO_2$ operators to inhibit yEGFP expression, which can be regulated by ATc. The inset cartoon is a simplified illustration of the network topology. (c) Stochastic (blue) and deterministic (green) simulation results for a simple GFP expression system, which are shown in the inset cartoon. It can be seen that stochastic simulation can generally follow deterministic dynamics but also show fluctuations. Numerical algorithms used to simulate such stochastic dynamics have been significantly improved over the past decade, mainly motivated by synthetic biology studies. (d) Cell fate determination can be visualized as a marble travelling in a rugged landscape. Local minima represent different cell fates and inherent noise can spontaneously push the marble from one minima to another. In this landscape, x_1 and x_2 represent protein abundances of different gene products and noise could lead to the transition from state A to state B. Based on Wang *et al.* (2015).[102]

feedback loop of comK and a degradation mechanism for the protease complex. The authors also derived a formula to describe how noise depended on mRNA transcription, protein translation and degradation rates. Based on this formula, the authors concluded that noise was inversely proportional to the transcription rate and not strongly influenced by the translation rate, which corresponded with experimental observations. Combined with the experimental results, the study indicated that intrinsic noise played a more important role than extrinsic noise. In addition, the study found that reducing noise in *comK* expression by changing its initial codon from *ATG* to *GTG* (lowering translational efficiency) could significantly decrease the percentage of competent cells. Similar findings have been shown by other studies exemplifying that noise could coordinate gene expression and enable probabilistic differentiation.[56,59,81]

Given its increased recognition, synthetic biologists have explored ways to tune and control gene expression noise. Murphy *et al.*[82] designed combinatorial promoters to characterize how operator sites would influence gene expression noise. Based on this, they later developed a novel method to control noise in synthetic gene networks in *S. cerevisiae*.[83] Specifically, the authors constructed a simple circuit where the bidirectional promoter *GAL10-GAL1* was used to drive *TetR* and green fluorescent protein (*yEGFP*) expression, but with *$TetO_2$* binding sites between the TATA box of the *GAL1* promoter and the yEGFP transcription start site so that yEGFP expression was regulated by the TetR repressor (Fig. 2b). The authors established five different yeast strains, designed with four different point mutations in the TATA box of the *GAL10* promoter. A mathematical model was developed and the modeling predictions were tested using flow cytometry measurements of yEGFP fluorescence. By combining the analysis of mathematical models and the collection of experimental data, the authors found that TATA box mutations could effectively reduce noise levels of a target gene with little influence on its dynamic range and basal expression.

Progress in understanding biological noise also helped revitalize interests in stochastic simulation and analysis.[84,85] First introduced in the 70's, the Gillespie algorithm[86] (glossary: stochastic simulation methods) was the standard approach for many years (Fig. 2c). Motivated by progress in synthetic biology studies of noise, the algorithm has been actively researched and improved.[87–94] Several novel mathematical models have been introduced to study the impact of noise in biological oscillations,[65] the cell cycle,[95,96] and multistable systems.[97–102] In particular, Tian *et al.*[99] proposed a systematic method to derive a stochastic model from a deterministic ODE using a slight modification. In this method, each deterministic variable in the ODE was replaced by a Poisson random variable within a small time interval and binomial random variables were used to approximate Poisson random variables in order to avoid negative values for molecular numbers in simulations.[103] Compared to previous stochastic methods,[86,87] the method proposed by Tian *et al.*[99] saved computational time by keeping the general description of biochemical reactions from the

deterministic model. In addition to above methods, Bratsun *et al.*[104] reformulated the Gillespie algorithm using time delays and formed master equations to explore delay issues in the stochastic process of gene regulation. Wang *et al.*[102] demonstrated that noise could benefit control in multistable systems by visualizing energy landscapes (Fig. 2d).

4 Oscillation

Oscillating behavior has been a long observed phenomenon in many biological systems.[105,106] For example, a circadian clock found in most living organisms from microbes to humans is maintained by endogenous oscillating biological processes to adapt to daily environmental alterations in the day/night cycle.[107] Cyanobacteria employ Kai proteins to produce sustainable oscillations to keep biological time and regulate cellular metabolism.[108] Mammalian neural oscillations play key roles in central nervous system functions, including information processing, sleep, and memory.[109] Moreover, owing to their dynamical properties, self-sustainable oscillators play important roles in some fundamental bioprocesses such as p53-mediated DNA damage responses,[110] NF-κB signaling transduction,[111] and Cdk1-APC/C driven cell cycle progression.[112]

However, the exact molecular mechanisms and non-linear dynamics of biological oscillators (natural periodic processes) remain largely unknown. Early work on biochemical oscillations mainly focused on discovering rather than probing oscillating phenomena.[113–117] A unifying scheme of oscillators in non-specialized regulatory networks had not been proposed until the blossom of synthetic biology in the early 2000s.[6,37,54,107,118] These synthetic gene circuits helped scientists to study the mechanisms generating oscillations in relatively simple contexts, but within highly dynamic systems. Feedback, especially negative feedback, is a general principle that has proven to be an indispensable requirement for generating oscillating behavior in protein concentrations[6,119–121] or cellular populations.[65,122–125] Here, we briefly introduce the negative-feedback oscillator and combined positive- and negative-feedback oscillator.

4.1 Negative-feedback oscillator

A negative-feedback loop is a common design feature found in genetic oscillators. In 2000, Elowitz and Leibler[6] constructed a synthetic oscillatory network, the "repressilator", in which three transcriptional repressors (LacI, TetR, and cI) inhibit each other by binding to their corresponding promoters. In this circuit, the TetR protein can inhibit *cI* expression, which in turn represses *LacI* transcription, and LacI can block *TetR* expression, forming a cyclic negative-feedback loop (Fig. 3a). The topology of the repressilator network enables periodic expression of each repressor protein in *E. coli*, resulting in oscillations with a period of ~150 minutes that can be transmitted to progenies. To build the repressilator, the authors first formulated a deterministic model with six coupled ODEs (glossary: ODE) to simulate the kinetic behavior of the three-gene system. The deterministic system has one unique steady state whose stability can be analyzed by using a bifurcation diagram. To investigate the influence of intrinsic noise, the authors used the Gillespie algorithm to perform stochastic

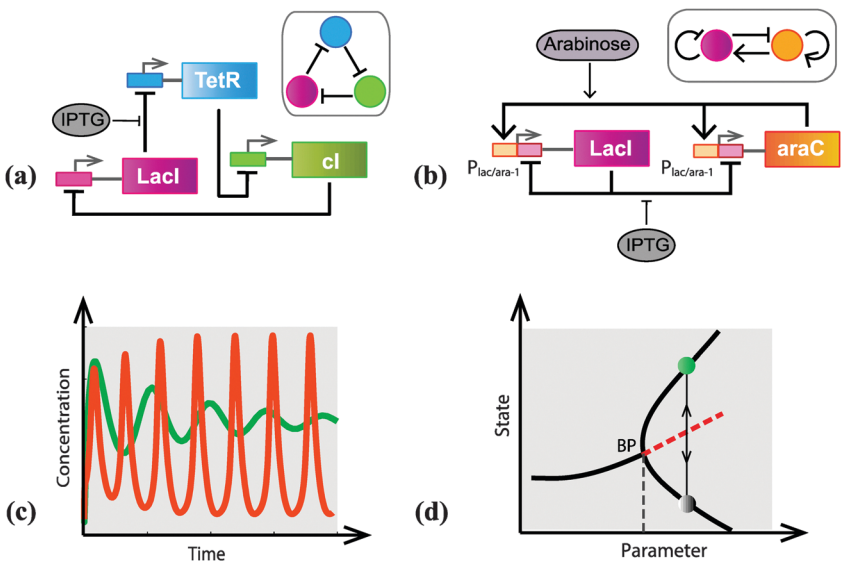

Fig. 3 Oscillations. (a) Simplified schematic of a negative-only feedback circuit based on Elowitz and Leibler (2000).[6] In this circuit, TetR inhibits cI, cI inhibits LacI, and LacI inhibits TetR, together forming a cyclic network. The inhibition from LacI to TetR can be regulated by IPTG. The inset cartoon represents a simplified diagram of this repressilator network. (b) Simplified schematic of a positive and negative feedback circuit based on Stricker *et al.* (2008).[119] In this circuit, *araC* and *LacI* are driven by a hybrid promoter ($P_{lac/ara-1}$) and form a positive and negative feedback. Inset cartoon is a simplified diagram of this dual-feedback oscillator. (c) Illustration of oscillating behavior in a negative-feedback circuit (green) and a positive- and negative-feedback circuit (orange). (d) Illustration of a typical Hopf bifurcation in oscillating systems. Here BP represents for the bifurcation point, after which is the oscillation region. The red dashed line indicates an unstable steady state. The green and grey circles illustrate an oscillatory reporter signal, where green means GFP on and grey represents a low fluorescence state.

simulations using parameter values similar to those used in the deterministic model. They found that their three-gene system could exhibit oscillations over a wide range of parameter values. Model predictions were later verified experimentally with dampened oscillations (Fig. 3c, green). As proof-of-concept work, this study demonstrated that oscillatory behavior could be realized by combining rational network design, *i.e.*, mathematical modeling, and genetic circuit engineering. Furthermore, Stricker and colleagues[119] discovered that a signal negative-feedback loop could also generate oscillations. The genetic circuit was constructed based on the LacI protein repressing its own expression by binding to its promoter $P_{lacO\text{-}1}$. This circuit was similar to a dual-feedback circuit we will discuss in Section 4.2. Experimental and computational results indicated that the single negative-feedback could also produce oscillations, but that it was difficult to tune the oscillation frequency. The simple circuit was also less responsive to IPTG inductions than the dual-feedback circuit and the presence of oscillations only occurred in a narrow range of inducer concentrations. Mathematical modelling analysis suggested that the negative-feedback circuit highly relied on a time delay to generate oscillating behavior.[126] In comparison, the repressilator harbored a relatively long time delay to realize periodic oscillations.

Moreover, negative feedback-based circuits could also be employed to generate population-level oscillations. For example, Balagaddé *et al.*[122] put forward a microfluidic bioreactor device to observe population dynamics of a synthetic circuit[27] in *E. coli*. The synthetic circuit consisted of a negative-feedback loop, which regulated the cell population. Then they found out that cell density had oscillating behavior and could be controlled by the circuit's states.

4.2 Positive- and negative-feedback oscillator

Negative-feedback loops can be engineered to generate autonomous oscillations. However, as it was shown with the repressilator, such oscillations tend not to be sustainable.[6] The search for robust oscillatory circuits started with mathematical and computational analyses[118] which indicated that a positive-feedback motif could promote robust and adjustable oscillations when coupled with negative-feedback loops. In addition, Tsai *et al.*[120] took the CDK1 oscillator in the *Xenopus* embryonic cell cycle as an example and performed large comparative studies between mathematical models with or without a positive-feedback loop. They identified a range of parameters in the model that could result in periodic behavior. The computational results revealed that the negative-feedback only version could yield oscillations but within a relatively small parameter range and poor adjustability in frequency. However, the positive-plus-negative feedback model achieved oscillations over a 4900-fold range of frequencies in the parameter range, indicating that the positive-feedback motif could significantly improve the oscillator's robustness and reliability.

In 2008, Stricker *et al.*[119] also developed a dual-feedback synthetic gene circuit that was demonstrated to be a tunable and robust oscillator in *E. coli*. In this circuit, a hybrid promoter $P_{lac/ara\text{-}1}$ was employed to drive the expression of the genes *araC*, *LacI*, and *GFP*. The expressed araC protein could activate $P_{lac/ara\text{-}1}$ transcription under arabinose induction and LacI protein could repress transcription in the absence of IPTG, together forming interlinked positive- and negative-feedback loops (Fig. 3b). Using a microfluidic device and time-lapse imaging, the authors could easily tune growth and induction conditions and monitor single-cell dynamic behavior of the oscillator in real-time. With inductions of arabinose and IPTG, more than 99% of cells observed displayed oscillations within several hours. Furthermore, the oscillator was remarkably robust (Fig. 3c, orange) over a wide range of inducer concentrations (IPTG or arabinose) and external growing conditions, such as temperature and media source. A mathematical model based on a previous theoretical design[118] was used to describe the biochemical reactions in the oscillator. The dynamic behavior of the model was explored using stochastic and deterministic simulations. These simulations were used to predict the relationship between the oscillation period and arabinose concentration. The modeling results indicated that oscillations could arise with increasing of doses of arabinose and that the oscillation period would be faster when using a low rather than high arabinose concentration. The authors then analyzed the dependence of reaction rates on temperature in the model to predict the relationship between temperature and the oscillation period. Similar to the negative-feedback only circuit, a time delay is also crucial to maintain oscillations in the dual-feedback circuit. By extending the mathematical model to include time delayed reactions, the authors were able to use bifurcation diagrams to analyze the robustness of the feedback loop by calculating the parameter region that would produce stable oscillations (Fig. 3d). Their numerical results showed that a time delay in the negative-feedback was a key design element for engineering a robust oscillator. The experimental results were consistent with the mathematical modeling analysis, further supporting these conclusions. Compared to the negative-feedback only circuit, both experimental and mathematical evidence have strongly suggested that the positive-feedback motif can contribute to the robustness and tunability of a genetic oscillator.

In many biological behaviors and processes, coordination of rhythmic behavior among individual elements in a complex community is a fundamental issue for homeostasis or even survival. Along these lines, Danino *et al.*[125] engineered synchronized oscillations in a population of cells. They used the positive- and negative-feedback oscillator circuit topology to construct a synchronized oscillation device by incorporating quorum-sensing components within a microfluidic platform. In this circuit, the promoter P_{luxI} drives the transcription of the *LuxI*, *aiiA* and *GFP* reporter genes. The synthase gene *LuxI* directs production of a small molecule AHL (3oxo-C6-HSL) that activates P_{luxI} when bound with LuxR protein, forming a positive-feedback loop. AiiA is an AHL protease that degrades the AHL molecule and hence negatively regulates the circuit. AHA molecules are produced inside the oscillator cells and diffuse in and out of bacterial cells, and are sensed by cells in neighboring chambers of the microfluidic device. Therefore, the intracellular concentration of AHL correlates with local cell density. The concentration of AHL

increases as the cell population grows and the P_{luxI} promoter will be activated once the cell density reaches a threshold, leading to a burst of *LuxI*, *aiiA* and *GFP* gene expression. However, increased levels of aiiA in turn degrade AHL and finally inactivate P_{luxI}. The role of AHL is to activate an intercellular signal to coordinate gene expression with nearby cells and thus generate a synchronized oscillator. Moreover, the oscillatory period and amplitude could be tuned by changing the flow rate in the main channel of the microfluidic device to control the degradation rate and effective AHL concentration. To give a quantitative understanding of the experimental results, the authors constructed a set of delay differential equation (DDE) models (glossary: DDE) to simulate the concentrations of LuxI, aiiA, internal and external AHL. A time delay was used to mimic the cascading processes of transcription and translation. This model was used to analyze the period of oscillations as a function of amplitude and flow rate. Furthermore, the model was extended to describe spatiotemporal patterns of GFP expression in a population of cells by coupling DDEs to a diffusion equation for AHL. The spatiotemporal model was able to display synchronization of spatiotemporal diffusion under different stochastic fluctuations as well as GFP expression wave propagation with different external AHL diffusion rates. The simulation results agreed well with experimental observations, suggesting that modeling is a useful approach to analyze dynamic spatiotemporal processes regulated by genetic circuits.

Later on, the same group engineered a more complicated dual-feedback circuit and realized global synchronization of thousands of oscillating colony "biopixels" at centimeter scale resolution through coupling quorum sensing with hydrogen peroxide (H_2O_2)-mediated redox signalling in *E. coli*.[127] In this circuit, the *LuxI* promoter drove the expression of *LuxI*, *aiiA*, and *ndh*, of which the first two gene products contributed to the formation of positive- and negative-feedback loops as in the previous example. The *ndh* gene encoded an enzyme to generate H_2O_2 vapour, which could also activate the *LuxI* promoter and hence constitute another positive feedback. The quorum-sensing machinery *LuxI* and *aiiA* enabled synchronized oscillations within a colony. H_2O_2, however, could pass through the microfluidic device and facilitate faster communication for coordination between colonies. Using this platform, they also constructed a liquid crystal display (LCD) in a microfluidic device. It is necessary to point out that in the oscillation system, controlling the protein or signal degradation rate is crucial for the oscillator to function. Either by using an ssrA tag for faster protein degradation or an external catalase to degrade H_2O_2, this work has shed light on the importance of a signal "queuing" mechanism for oscillator synchrony.[128] Furthermore, Chen *et al.*[129] recently constructed a robust oscillating system within a synthetic microbial consortium using two strains of cells with different gene circuits (an activator and a repressor strain) that combined to make positive- and negative-feedback loops.

The positive- and negative-feedback topology has also been successfully used to generate robust oscillations in mammalian cells. Tigges *et al.*[121] engineered a synthetic mammalian oscillator circuit using a sense–antisense regulation mechanism. In this circuit, the promoter $P_{hCMV*\text{-}1}$ and P_{PIR} drive the sense and antisense expression of tetracycline-dependent transactivator (tTA), respectively. tTA auto-activates $P_{hCMV*\text{-}1}$ transcription, forming a positive-feedback, while PIT (pristinamycin-dependent transactivator) driven by $P_{hCMV*\text{-}1}$ induces P_{PIR} activation, leading to the antisense transcription of tTA and the negative regulation of tTA expression. The linking of positive- and negative-feedbacks in this circuit enabled autonomous and sustainable oscillations with a period of 170 ± 71 min for more than 20 hours in Chinese hamster ovary cells. Furthermore, the mammalian oscillator could be fine-tuned by varying the transfected DNA doses to change the frequency and amplitude. Interestingly, the oscillating cells showed considerable variability in timing and amplitude, suggesting that gene expression noise may shape this dynamic process. The authors validated this concept using a deterministic mathematical model for the expression of tTA, PIT, and GFP. They then modified this model to incorporate time delays for tetracycline and interactions between sense–antisense expression units by adding a diffusion process and assuming that the occupancy of RNA polymerases would change the transcription probability. The authors used Monte Carlo simulations (glossary: stochastic simulation methods) to find parameter sets that could lead to oscillatory behaviors. The oscillation frequency predicted by the refined deterministic model agreed well with the experimentally observed oscillation period. To consider the influence of intrinsic noise, the authors proposed a stochastic model and used a generalized Binomial τ-leap algorithm (Bτ-DSSA),[91] which included a time delay to increase the efficiency of multi-cellular calculation. Their stochastic simulation results recapitulated the patterns of cell–cell variability seen in experimental data and confirmed the importance of stochastic effects.

5 Cell–cell communication and pattern formation

Cell–cell communication exists in unicellular and multicellular species, and is responsible for coordinating collective population behaviors, such as biofilm formation,[130] cell differentiation[40] and vertebrate embryonic development.[131] Before synthetic biology, cell–cell communication mainly focused on synaptic transmission[132] and cellular signal processing.[133] Recently, the use of molecular components and devices for cell–cell communication has enabled synthetic engineering of more complex circuits to investigate cell–cell interactions and phenomena at higher levels of biological organization, such as population decision-making and behaviors.

Quorum sensing (QS) is a widespread cell–cell communication mechanism in the bacteria world,[134] such as the LuxR/LuxI system in *Vibrio fischeri* and the LasR/LasI system in *Pseudomonas aeruginosa*. So far, quorum-sensing mechanisms, coupled with engineering principles, have been employed to program population control,[27,132,135–139] build synchronized oscillations,[125,128,140] produce diverse cell phenotypes,[141,142] control biofilm signaling,[130] produce pattern formation,[80,143–146] and to construct synthetic

ecosystems.[123] Here, we mainly review the representative studies that integrate mathematical reasoning with experimental validation to probe mechanisms involved in pattern formation and cell–cell communication.

In 2005, Basu *et al.*[145] programmed a synthetic multicellular system to form bullseye, ellipse, heart, and clover patterns based on local AHL gradients around sender cells (Fig. 4a). Morphogen diffusion on the solid plate established a natural gradient that could be sensed by receiver cells and induced differential responses at distinct regions. The authors built a system of five ODEs to model a single cell's response to AHL and performed spatiotemporal simulations of AHL diffusion and intercellular communication. By combining mathematical modeling and experimental evidence, this study provided us with a better understanding of the multi-scale mechanisms underlying pattern formation in development.

In a recent study from the You group,[143] a novel pattern forming mechanism was developed using a synthetic gene circuit in *E. coli*. This circuit is composed of an auto-activating motif driven by the activator T7 RNAP and negative regulation of the activator induced by AHL from a positive-feedback module (Fig. 4b). Bacteria harbouring this circuit generated a self-organized ring pattern. An agent-based computational model was further developed to simulate the spatiotemporal dynamics. In the simulation, cells on a grid were assumed to have identical concentrations of intracellular T7 RNAP and lysozyme and, at each time step, a cell division or movement event was chosen randomly with equal probability. The simulation results suggested that a robust pattern is not dependent on morphogen gradients, but rather these gradients act as a timing cue to initiate pattern formation and maintenance. This research sheds light on a novel morphogen timing mechanism to generate spatial patterns in developmental processes.

To date, diverse mechanisms have been proposed about how cells produce spatial patterns, either dependent on or independent of morphogen gradients. Liu *et al.*[146] recently used synthetic approaches to reveal another mechanism that could generate spatial patterns by coupling cell motility with density. The authors engineered a synthetic gene circuit having two modules: the constitutively expressed LuxR/LuxI system to monitor local cell density (density-sensing module), and a module with LuxR/LuxI regulating *cheZ* expression to control cell motility (motility-control module). At high cell densities, the LuxR–AHL complex would inhibit *cheZ* transcription, resulting in a loss of motility. However, cheZ reintroduction made cells regain motility at low cell densities. When placed in the middle of semi-solid agar plates, the engineered *E. coli* automatically and sequentially developed periodic stripes with alternating high and low cell densities as cells moved radially outwards. The authors also used modeling to investigate this self-organized

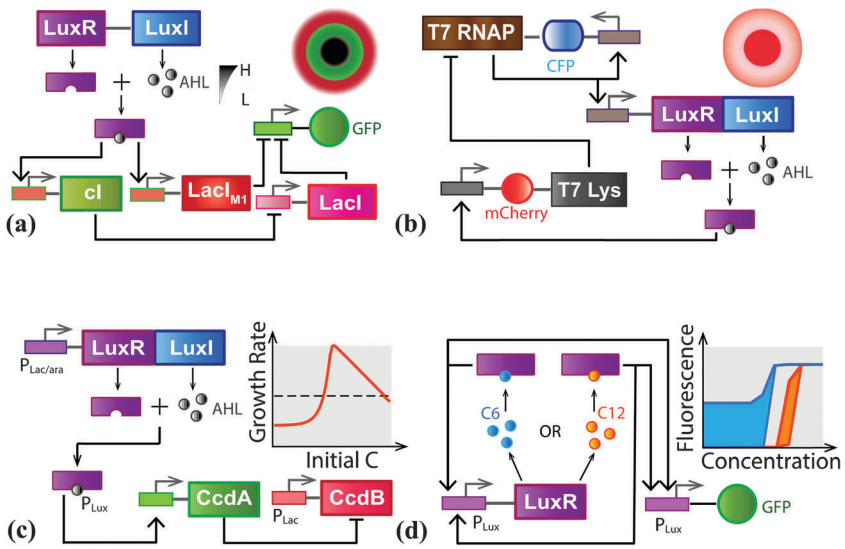

Fig. 4 Cell–cell communication. (a) Illustration of a gene circuit that can produce a bullseye pattern based on Basu *et al.* (2005).[145] This circuit has three operations in different AHL concentrations with initiation of the LuxI–LuxR complex. When AHL concentration is low, LacI represses GFP expression; when AHL concentration is medium, GFP is expressed; when AHL concentration is high, LacI$_{M1}$ represses GFP. The inset cartoon shows the bullseye pattern. (b) Illustration of a gene circuit that can produce a self-organized pattern based on Payne *et al.* (2013).[143] The circuit consists of two parts: an activation part containing a positive feedback loop with T7 RNA polymerase (T7 RNAP) and an inhibition part of quorum sensing-mediated lysozyme expression. Specifically, T7 RNAP self-activates itself as well as *LuxR* and *LuxI* expressions, and the two gene product LuxR–AHL complex then induces T7 lysozyme (T7 Lys) expression. T7 Lys then inhibits T7 RNAP. The dynamics is reported by mCherry and CFP. The inset cartoon illustrates the self-organized ring pattern. (c) Illustration of the Allee effect in a programmed circuit and the growth rate of an engineered bacterial population based on Smith *et al.* (2014).[138] In the circuit, the $P_{Lac/ara}$ promoter controls the LuxR and LuxI quorum sensing (QS) system. In the presence of AHL, the QS system activates CcdA. Then CcdA inhibits CcdB, which will lead to cell death. The inset cartoon is a simulation result of the Allee effect. (d) Illustration of the crosstalk circuit based on Wu *et al.* (2014).[79] LuxR protein driven by P_{Lux} is bound by AHL molecules (C6 or C12), and the complex further activates P_{Lux}, forming a positive feedback. GFP is used as a reporter for LuxR dynamics. The inset cartoon represents the bistable region under C6 (blue) and C12 (yellow) induction. C6: 3oxo-C6-HSL; C12: 3oxo-C12-HSL.

pattern formation. A random walk was used to model the motion of cells and the logistic equation was used to model population growth and saturation. Fisher's propagation diffusion equation[147,148] with an additional drift term was used to capture the effect of chemotaxis and the nutrient concentration was coupled to cell density. Parameter values were estimated using relevant literature and experimental data. With these above assumptions, a spatiotemporal profile for the cell population was generated. Moreover, to gain a deeper understanding, the dependence of cell motility on density was considered in a basic Fisher's equation. In order to circumvent instabilities of wavelength in the modified diffusion equation, the rate of AHL was used as a signal in cell density. A nutrient field was also included in the modified model to avoid the cell saturation problem. The mathematical model integrating diffusion-like equations with logistic equations suggested that the autonomous stripe pattern is produced from a recurrent aggregation of AHL molecules at the propagating front of the expanding cell population. Further experiments showed that the number of stripes could be manipulated by tuning expression in the genetic circuit. This study reveals that a recurrent spatial structure can be generated by tuning the cell's motility and density, which may provide novel insights for developmental systems.

Another example in which the relationship between an individual cell and a population of cells was explored was performed by Smith *et al.* In this study, the authors built a synthetic circuit integrating LuxR/LuxI QS and CcdA/CcdB toxin–antitoxin system to investigate the Allee effect in bacteria, a common biological phenomenon describing the relationship between population density and individual fitness (Fig. 4c). In this circuit, IPTG induces *LuxR* and *LuxI* expression, as well as the cell-killing protein CcdB. LuxI directs the synthesis of AHL, which can bind the LuxR protein and activate the expression of the cell-rescuing protein CcdA when the cell density exceeds a threshold. To understand the behavior of this system, the authors built a mathematical model of five DDEs to simulate bacterial density under different concentrations of CcdA, CcdB and AHL. The five-DDE system was then simplified to two DDEs on bacterial density and AHL concentration. The model was parameterized using data collected in previous studies and new experiments. The authors extended the DDE model to examine the impact of leaky AHL expression, the metabolic burden of AHL, and nonlinear CcdA synthesis. They found out that if these three factors were in a certain range, they would not have substantial influence on experimental results, exemplifying the sufficiency of the simple model to describe the dynamics of the genetic circuit. The DDE model was later modified to describe stochastic dynamics by adding white noise (glossary: stochastic simulation methods) and making the cell density threshold probabilistic. The models (DDE and Stochastic) agreed with experimental results and showed that a strong Allee effect resulted in a trade-off between population spread and survival for a cooperative species: a high dispersal rate benefits spread, but also increases the risk that the population fails to invade or might even go extinct. By combing theoretical analysis and experimental observation, this study provided a novel understanding of the mechanisms affecting bacterial spread and may be helpful for exploring novel interventions to treat infectious diseases.

QS based cell–cell communication has also been found to induce unexpected host–circuit interactions. Recently, Wu and colleagues[79] systematically characterized crosstalk between LuxR/LuxI and LasR/LasI systems and found that QS crosstalk can be decomposed into signal crosstalk and promoter crosstalk. Furthermore, different crosstalk mechanisms could be engineered to generate distinct population dynamics from unimodality to bimodality using positive-feedback loops. Under the guidance of stochastic simulation, the authors found that promoter crosstalk could exhibit trimodal responses due to crosstalk-induced mutations. Signal crosstalk instead significantly decreases the circuit's bistable potential while maintaining unimodality (Fig. 4d). This study suggested that intercellular communication specificity was limited in bacteria and that crosstalk might be widespread in single organisms given the high prevalence of QS mechanisms.

Mathematical modeling has also been used to explain and direct the study of multicellular QS generated phenomena, such as bidirectional communication mediated biofilm formation. Brenner *et al.*[130] designed a microbial consensus consortium (MCC) network comprised of two groups of cells, in which Circuit A in group I cells synthesize 3oxo-C12-HSL molecules, and Circuit B in group II cells produce C4-HSL molecules. 3oxo-C12-HSL can be sensed by group II cells and activate C4-HSL expression, while C4-HSL can induce 3oxo-C12-HSL synthesis in group I. At sufficient population densities, the two auto-inducers would promote the corresponding circuit's activation and lead to a MCC response in which the two microbial populations could communicate with each other and coordinate gene expression. The full MCC was modeled with a system of four ODEs. The authors obtained a possible threshold for obtaining a consensus response by solving the equations analytically. The modeling results indicated that both groups' feedback designs exhibited higher levels of expression within the presence of each other. This finding confirmed experimental results showing that when two groups of cells grow together, a sustained consensual consortium was developed in engineered bacterial biofilms. As expected, such multicellular systems may contribute to our understanding of the interactions, cooperation and formation of pathogenic biofilms.

In addition to QS based cell–cell communication, other mechanisms have been explored to engineer microbe consortiums. In particular, Momeni *et al.*[149] used *S. cerevisiae* strains to show the fitness effect of exchanging essential metabolites in a spatial environment, which was based on a metabolic/auxotrophic cross-feeding interaction. They set up a community using randomly distributed yeast with three colored strains, which represent different interaction strategies: competition, cooperation, and cheating. Without adenine and lysine supplements, the cooperation interaction strain dominated. However, under the condition of adenine and lysine supplements, pure competition leads to three evenly distributed strains. An extended diffusion model was then used to simulate this organized pattern formation. Together with experimental results, the authors argued that

cheaters, who contributed less and received less from self-organization, were isolated in a shared resource environment. With an abundance of nutrition, cells were forced to grow upward and the three strains obtained an equal chance of survival.

6 Conclusions

Gene regulatory networks are central to the fundamental mechanisms regulating cell function and behavior. Previous studies suggested that transcriptional network dynamics largely influence and control differential gene expression and developmental patterns. However, investigations of such processes in natural systems are usually confounded by the complex contexts and other unknown interactions that may affect such networks. Alternatively, building synthetic gene networks from the bottom up provides a unique approach to confront this challenge. With the help of synthetic biology strategies, we have made inroads into this problem with the hope of better understanding cell development.[150] Mathematical modeling complements the toolbox of synthetic biology by enhancing the capacity to predict and explore the behavior of unbuilt gene circuits and multicellular systems. The presence of feedbacks and stochasticity can make the logic of GRNs non-intuitive, thus, simulating these systems in a "dry lab" setting can enable the exploration of a high dimensional space of possibilities which would have otherwise been time consuming or costly in a purely wet lab setting. Similarly, the current state of synthetic multicellular consortia, which consists of two or three distinct cell populations, gives us a better understanding of how cells communicate and synchronize with each other.

In this review, we briefly discussed how synthetic biology approaches in the past 15 years have helped inform our understanding of gene regulation and complex cell behaviors. Specifically, we highlighted examples combining synthetic gene networks and mathematical modelling to understand four fundamental mechanisms: multistability, stochastic gene expression, oscillations, and cell–cell communication. The creation of small artificial networks opens a novel window to decipher naturally occurring complexity. Furthermore, with the increasing development of more reliable and interoperable devices as well as effective design principles, we will be able to engineer higher-order networks and systems to probe the mechanisms underlying cell differentiation and multicellularity, the development of microbial consortia, and cellular evolution.

Glossary

Ordinary differential equation (ODE)
: An ODE is a dynamical system equation consisting of functions with only one independent variable. It is a convenient tool for modeling interactions among genetic circuit components.[151,152] Some ODEs can be solved analytically to obtain steady states, while in most cases, the equations can only be solved using numerical algorithms such as Runge–Kutta methods, which are already embedded in popular software and programming languages like MATLAB and Python.

Delay differential equation (DDE)
: A DDE is an equation with functions that rely on a delayed time coordinate. The steps method with a given initial condition is used to obtain numerical solutions.

Stochastic simulation methods
: One important method to simulate stochastic biochemical reactions is the Gillespie algorithm[86] and related improved algorithms.[87,89] The Gillespie algorithm was first applied in modeling chemical reactions and later widely used in synthetic biology. Another method to build a stochastic model is based on a Brownian motion process. In signal and communication fields, engineers use a Wiener process to generate Gaussian white noise[153] in order to simulate environmental noise. In addition to the above methods, Monte Carlo algorithms, which are based on randomly repeated sampling, are another popular methodology employed to simulate a physical environment or mathematical model with noise.

Bifurcation diagram
: A bifurcation diagram is a dynamical system analysis tool that can give a visualization of a system's dynamical behavior. It is a method to illustrate the equilibria or orbits of a system as a function of a changing parameter.[154] In synthetic biology, two kinds of bifurcations are widely used, the saddle-node bifurcation and the Hopf bifurcation. A saddle-node bifurcation, also called a fold bifurcation, describes the creation or annihilation of two fixed points and has been applied in toggle structures. The Hopf bifurcation, which is found in many oscillatory systems, can represent the transition between a limit cycle or oscillation and an equilibrium point. *Hysteresis* occurs when two attractors (equilibria) coexist at the same parameter value. Thus, in a system with hysteresis, changing a parameter from p_1 to p_2 can change the system from state S_1 to state S_2, but changing the parameter back to p_1 may not return the system back to state S_1.

Energy landscape
: Attractor and stability theory provides a realistic framework to study nonlinear system dynamics.[155] In dynamical systems, the quasi-potential energy landscape proposed by Waddington[31] has been widely applied to characterize the stability of a system. In general, the landscape potential (U) is defined as ($U = -\ln P$), where P is the probability of attractor states.[99] Similarly, in synthetic gene networks with multiple steady states, different cell types correspond to different attractor states, and the differentiation path between each cell is represented by the transition between each attractor.[156] In simulation, the weighted-ensemble algorithm[157,158] based on random walks is widely used to numerically obtain pseudo potential energy landscapes.

Acknowledgements

We thank members of Xiao Wang's lab for helpful discussions and suggestions. F. W. was supported by American Heart Association Predoctoral Fellowship. X. W. was supported by National Science Foundation Grant DMS-1100309 and National Institutes of Health Grant GM106081. Y.-C. L. was supported by ARO under Grant No. W911NF-14-1-0504.

References

1 D. G. Gibson, G. A. Benders, C. Andrews-Pfannkoch, E. A. Denisova, H. Baden-Tillson, J. Zaveri, T. B. Stockwell, A. Brownley, D. W. Thomas, M. A. Algire, C. Merryman, L. Young, V. N. Noskov, J. I. Glass, J. C. Venter, C. A. Hutchison and H. O. Smith, *Science*, 2008, **319**, 1215–1220.
2 J. Cello, A. V. Paul and E. Wimmer, *Science*, 2002, **297**, 1016–1018.
3 A. S. Khalil, T. K. Lu, C. J. Bashor, C. L. Ramirez, N. C. Pyenson, J. K. Joung and J. J. Collins, *Cell*, 2012, **150**, 647–658.
4 K. Standage-Beier, Q. Zhang and X. Wang, *ACS Synth. Biol.*, 2015, **4**, 1217–1225.
5 T. S. Gardner, C. R. Cantor and J. J. Collins, *Nature*, 2000, **403**, 339–342.
6 M. B. Elowitz and S. Leibler, *Nature*, 2000, **403**, 335–338.
7 A. A. Green, P. A. Silver, J. J. Collins and P. Yin, *Cell*, 2014, **159**, 925–939.
8 D. G. Gibson, J. I. Glass, C. Lartigue, V. N. Noskov, R.-Y. Chuang, M. A. Algire, G. A. Benders, M. G. Montague, L. Ma, M. M. Moodie, C. Merryman, S. Vashee, R. Krishnakumar, N. Assad-Garcia, C. Andrews-Pfannkoch, E. A. Denisova, L. Young, Z.-Q. Qi, T. H. Segall-Shapiro, C. H. Calvey, P. P. Parmar, C. A. Hutchison, H. O. Smith and J. C. Venter, *Science*, 2010, **329**, 52–56.
9 N. Annaluru, H. Muller, L. A. Mitchell, S. Ramalingam, G. Stracquadanio, S. M. Richardson, J. S. Dymond, Z. Kuang, L. Z. Scheifele, E. M. Cooper, Y. Cai, K. Zeller, N. Agmon, J. S. Han, M. Hadjithomas, J. Tullman, K. Caravelli, K. Cirelli, Z. Guo, V. London, A. Yeluru, S. Murugan, K. Kandavelou, N. Agier, G. Fischer, K. Yang, J. A. Martin, M. Bilgel, P. Bohutskyi, K. M. Boulier, B. J. Capaldo, J. Chang, K. Charoen, W. J. Choi, P. Deng, J. E. DiCarlo, J. Doong, J. Dunn, J. I. Feinberg, C. Fernandez, C. E. Floria, D. Gladowski, P. Hadidi, I. Ishizuka, J. Jabbari, C. Y. L. Lau, P. A. Lee, S. Li, D. Lin, M. E. Linder, J. Ling, J. Liu, J. Liu, M. London, H. Ma, J. Mao, J. E. McDade, A. McMillan, A. M. Moore, W. C. Oh, Y. Ouyang, R. Patel, M. Paul, L. C. Paulsen, J. Qiu, A. Rhee, M. G. Rubashkin, I. Y. Soh, N. E. Sotuyo, V. Srinivas, A. Suarez, A. Wong, R. Wong, W. R. Xie, Y. Xu, A. T. Yu, R. Koszul, J. S. Bader, J. D. Boeke and S. Chandrasegaran, *Science*, 2014, **344**, 55–58.
10 A. J. Keung, C. J. Bashor, S. Kiriakov, J. J. Collins and A. S. Khalil, *Cell*, 2014, **158**, 110–120.
11 J. G. Zalatan, M. E. Lee, R. Almeida, L. A. Gilbert, E. H. Whitehead, M. La Russa, J. C. Tsai, J. S. Weissman, J. E. Dueber, L. S. Qi and W. A. Lim, *Cell*, 2015, **160**, 339–350.
12 F. Wu and X. Wang, *Sci. Prog.*, 2015, **98**, 244–252.
13 J. L. Fortman, S. Chhabra, A. Mukhopadhyay, H. Chou, T. S. Lee, E. Steen and J. D. Keasling, *Trends Biotechnol.*, 2008, **26**, 375–381.
14 A. S. Khalil and J. J. Collins, *Nat. Rev. Genet.*, 2010, **11**, 367–379.
15 P. Redondo, J. Prieto, I. G. Muñoz, A. Alibés, F. Stricher, L. Serrano, J.-P. Cabaniols, F. Daboussi, S. Arnould, C. Perez, P. Duchateau, F. Pâques, F. J. Blanco and G. Montoya, *Nature*, 2008, **456**, 107–111.
16 I. G. Muñoz, J. Prieto, S. Subramanian, J. Coloma, P. Redondo, M. Villate, N. Merino, M. Marenchino, M. D'Abramo, F. L. Gervasio, S. Grizot, F. Daboussi, J. Smith, I. Chion-Sotinel, F. Pâques, P. Duchateau, A. Alibés, F. Stricher, L. Serrano, F. J. Blanco and G. Montoya, *Nucleic Acids Res.*, 2011, **39**, 729–743.
17 S. Galanie, K. Thodey, I. J. Trenchard, M. F. Interrante and C. D. Smolke, *Science*, 2015, **349**, 1095–1100.
18 K. Pardee, A. A. Green, T. Ferrante, D. E. Cameron, A. DaleyKeyser, P. Yin and J. J. Collins, *Cell*, 2014, **159**, 940–954.
19 M. Amidi, M. de Raad, D. J. A. Crommelin, W. E. Hennink and E. Mastrobattista, *Syst. Synth. Biol.*, 2010, **5**, 21–31.
20 J. R. Coleman, D. Papamichail, S. Skiena, B. Futcher, E. Wimmer and S. Mueller, *Science*, 2008, **320**, 1784–1787.
21 S. Slomovic and J. J. Collins, *Nat. Methods*, 2015, **12**, 1085–1090.
22 F. Farzadfard and T. K. Lu, *Science*, 2014, **346**, 1256272.
23 K. Takahashi, K. Tanabe, M. Ohnuki, M. Narita, T. Ichisaka, K. Tomoda and S. Yamanaka, *Cell*, 2007, **131**, 861–872.
24 L. Warren, P. D. Manos, T. Ahfeldt, Y.-H. Loh, H. Li, F. Lau, W. Ebina, P. K. Mandal, Z. D. Smith, A. Meissner, G. Q. Daley, A. S. Brack, J. J. Collins, C. Cowan, T. M. Schlaeger and D. J. Rossi, *Cell Stem Cell*, 2010, **7**, 618–630.
25 I. Weissman, *Cell Stem Cell*, 2012, **10**, 663–665.
26 Y. Yokobayashi, R. Weiss and F. H. Arnold, *Proc. Natl. Acad. Sci. U. S. A.*, 2002, **99**, 16587–16591.
27 L. You, R. S. Cox, R. Weiss and F. H. Arnold, *Nature*, 2004, **428**, 868–871.
28 J. M. Pedraza and A. van Oudenaarden, *Science*, 2005, **307**, 1965–1969.
29 M. Elowitz and W. A. Lim, *Nature*, 2010, **468**, 889–890.
30 S. Mukherji and A. van Oudenaarden, *Nat. Rev. Genet.*, 2009, **10**, 859–871.
31 C. H. Waddington and others, *Strategy Genes Discuss. Some Asp. Theor. Biol. Append.* H Kacser, 1957, pp. ix+–262.
32 B. D. MacArthur, A. Ma'ayan and I. R. Lemischka, *Nat. Rev. Mol. Cell Biol.*, 2009, **10**, 672–681.
33 S. A. Kauffman, *J. Theor. Biol.*, 1969, **22**, 437–467.
34 S. Huang and D. E. Ingber, *Cancer Cell*, 2005, **8**, 175–176.
35 S. Manu, S. Surkova, A. V. Spirov, V. V. Gursky, H. Janssens, A.-R. Kim, O. Radulescu, C. E. Vanario-Alonso, D. H. Sharp,

M. Samsonova and J. Reinitz, *PLoS Comput. Biol.*, 2009, **5**, e1000049.
36 W. Xiong and J. E. Ferrell, *Nature*, 2003, **426**, 460–465.
37 J. R. Pomerening, E. D. Sontag and J. E. Ferrell, *Nat. Cell Biol.*, 2003, **5**, 346–351.
38 B. P. Kramer, A. U. Viretta, M. D.-E. Baba, D. Aubel, W. Weber and M. Fussenegger, *Nat. Biotechnol.*, 2004, **22**, 867–870.
39 M. Wu, R.-Q. Su, X. Li, T. Ellis, Y.-C. Lai and X. Wang, *Proc. Natl. Acad. Sci. U. S. A.*, 2013, **110**, 10610–10615.
40 A. Becskei, *EMBO J.*, 2001, **20**, 2528–2535.
41 M. S. Antunes, K. J. Morey, J. J. Smith, K. D. Albrecht, T. A. Bowen, J. K. Zdunek, J. F. Troupe, M. J. Cuneo, C. T. Webb, H. W. Hellinga and J. I. Medford, *PLoS One*, 2011, **6**, e16292.
42 J. J. Tabor, A. Levskaya and C. A. Voigt, *J. Mol. Biol.*, 2011, **405**, 315–324.
43 H. Kobayashi, M. Kærn, M. Araki, K. Chung, T. S. Gardner, C. R. Cantor and J. J. Collins, *Proc. Natl. Acad. Sci. U. S. A.*, 2004, **101**, 8414–8419.
44 T. Ellis, X. Wang and J. J. Collins, *Nat. Biotechnol.*, 2009, **27**, 465–471.
45 J. E. Ferrell Jr., J. R. Pomerening, S. Y. Kim, N. B. Trunnell, W. Xiong, C.-Y. F. Huang and E. M. Machleder, *FEBS Lett.*, 2009, **583**, 3999–4005.
46 H. Y. Kueh, A. Champhekar, S. L. Nutt, M. B. Elowitz and E. V. Rothenberg, *Science*, 2013, **341**, 670–673.
47 K. E. Lee, J. Seo, J. Shin, E. H. Ji, J. Roh, J. Y. Kim, W. Sun, J. Muhr, S. Lee and J. Kim, *Proc. Natl. Acad. Sci. U. S. A.*, 2014, **111**, 2794–2799.
48 D. P. S. Osborn, K. Li, Y. Hinits and S. M. Hughes, *Dev. Biol.*, 2011, **350**, 464–475.
49 D.-E. Chang, S. Leung, M. R. Atkinson, A. Reifler, D. Forger and A. J. Ninfa, *Proc. Natl. Acad. Sci. U. S. A.*, 2010, **107**, 175–180.
50 A. Einstein, *Ann. Phys.*, 1905, **322**, 549–560.
51 C. E. Shannon, *Bell Syst. Tech. J.*, 1948, **27**, 379–423.
52 E. N. Lorenz, *J. Atmos. Sci.*, 1969, **26**, 636–646.
53 J. P. Crutchfield, J. D. Farmer and B. A. Huberman, *Phys. Rep.*, 1982, **92**, 45–82.
54 M. B. Elowitz, A. J. Levine, E. D. Siggia and P. S. Swain, *Science*, 2002, **297**, 1183–1186.
55 E. M. Ozbudak, M. Thattai, I. Kurtser, A. D. Grossman and A. van Oudenaarden, *Nat. Genet.*, 2002, **31**, 69–73.
56 W. J. Blake, M. KÆrn, C. R. Cantor and J. J. Collins, *Nature*, 2003, **422**, 633–637.
57 J. M. Raser and E. K. O'Shea, *Science*, 2004, **304**, 1811–1814.
58 A. Colman-Lerner, A. Gordon, E. Serra, T. Chin, O. Resnekov, D. Endy, C. Gustavo Pesce and R. Brent, *Nature*, 2005, **437**, 699–706.
59 J. R. Chabot, J. M. Pedraza, P. Luitel and A. van Oudenaarden, *Nature*, 2007, **450**, 1249–1252.
60 Y. Buganim, D. A. Faddah, A. W. Cheng, E. Itskovich, S. Markoulaki, K. Ganz, S. L. Klemm, A. van Oudenaarden and R. Jaenisch, *Cell*, 2012, **150**, 1209–1222.
61 H. H. Chang, M. Hemberg, M. Barahona, D. E. Ingber and S. Huang, *Nature*, 2008, **453**, 544–547.
62 D. W. Austin, M. S. Allen, J. M. McCollum, R. D. Dar, J. R. Wilgus, G. S. Sayler, N. F. Samatova, C. D. Cox and M. L. Simpson, *Nature*, 2006, **439**, 608–611.
63 Y. Dublanche, K. Michalodimitrakis, N. Kümmerer, M. Foglierini and L. Serrano, *Mol. Syst. Biol.*, 2006, **2**, 41.
64 N. Rosenfeld, J. W. Young, U. Alon, P. S. Swain and M. B. Elowitz, *Science*, 2005, **307**, 1962–1965.
65 Y. Tanouchi, A. Pai, H. Park, S. Huang, R. Stamatov, N. E. Buchler and L. You, *Nature*, 2015, **523**, 357–360.
66 M. Acar, J. T. Mettetal and A. van Oudenaarden, *Nat. Genet.*, 2008, **40**, 471–475.
67 G. Balázsi, A. van Oudenaarden and J. J. Collins, *Cell*, 2011, **144**, 910–925.
68 A. Raj and A. van Oudenaarden, *Cell*, 2008, **135**, 216–226.
69 R. Losick and C. Desplan, *Science*, 2008, **320**, 65–68.
70 G. M. Süel, J. Garcia-Ojalvo, L. M. Liberman and M. B. Elowitz, *Nature*, 2006, **440**, 545–550.
71 A. Raj, S. A. Rifkin, E. Andersen and A. van Oudenaarden, *Nature*, 2010, **463**, 913–918.
72 N. J. Guido, X. Wang, D. Adalsteinsson, D. McMillen, J. Hasty, C. R. Cantor, T. C. Elston and J. J. Collins, *Nature*, 2006, **439**, 856–860.
73 N. J. Guido, P. Lee, X. Wang, T. C. Elston and J. J. Collins, *Biophys. J.*, 2007, **93**, L55–L57.
74 J. C. W. Locke, J. W. Young, M. Fontes, M. J. H. Jiménez and M. B. Elowitz, *Science*, 2011, **334**, 366–369.
75 A. Eldar, V. K. Chary, P. Xenopoulos, M. E. Fontes, O. C. Losón, J. Dworkin, P. J. Piggot and M. B. Elowitz, *Nature*, 2009, **460**, 510–514.
76 A. Presser, M. B. Elowitz, M. Kellis and R. Kishony, *Proc. Natl. Acad. Sci. U. S. A.*, 2008, **105**, 950–954.
77 C. Gonzalez, J. C. J. Ray, M. Manhart, R. M. Adams, D. Nevozhay, A. V. Morozov and G. Balazsi, *Mol. Syst. Biol.*, 2015, **11**, 827.
78 E. M. Ozbudak, M. Thattai, H. N. Lim, B. I. Shraiman and A. van Oudenaarden, *Nature*, 2004, **427**, 737–740.
79 F. Wu, D. J. Menn and X. Wang, *Chem. Biol.*, 2014, **21**, 1629–1638.
80 H. Maamar, A. Raj and D. Dubnau, *Science*, 2007, **317**, 526–529.
81 A. Eldar and M. B. Elowitz, *Nature*, 2010, **467**, 167–173.
82 K. F. Murphy, G. Balázsi and J. J. Collins, *Proc. Natl. Acad. Sci. U. S. A.*, 2007, **104**, 12726–12731.
83 K. F. Murphy, R. M. Adams, X. Wang, G. Balázsi and J. J. Collins, *Nucleic Acids Res.*, 2010, **38**, 2712–2726.
84 J. Paulsson, *Nature*, 2004, **427**, 415–418.
85 M. Kærn, T. C. Elston, W. J. Blake and J. J. Collins, *Nat. Rev. Genet.*, 2005, **6**, 451–464.
86 D. T. Gillespie, *J. Phys. Chem.*, 1977, **81**, 2340–2361.
87 D. T. Gillespie, *J. Chem. Phys.*, 2001, **115**, 1716–1733.
88 Y. Cao, D. T. Gillespie and L. R. Petzold, *J. Chem. Phys.*, 2007, **126**, 224101.
89 D. T. Gillespie, *Annu. Rev. Phys. Chem.*, 2007, **58**, 35–55.
90 R. Erban, I. G. Kevrekidis, D. Adalsteinsson and T. C. Elston, *J. Chem. Phys.*, 2006, **124**, 084106.
91 A. Leier, T. T. Marquez-Lago and K. Burrage, *J. Chem. Phys.*, 2008, **128**, 205107.

92 M. A. Gibson and J. Bruck, *J. Phys. Chem. A*, 2000, **104**, 1876–1889.
93 D. Adalsteinsson, D. McMillen and T. C. Elston, *BMC Bioinf.*, 2004, **5**, 24.
94 X. Wang, B. Errede and T. C. Elston, *Biophys. J.*, 2008, **94**, 2017–2026.
95 Y. Zhang, M. Qian, Q. Ouyang, M. Deng, F. Li and C. Tang, *Phys. D*, 2006, **219**, 35–39.
96 F. Li, T. Long, Y. Lu, Q. Ouyang and C. Tang, *Proc. Natl. Acad. Sci. U. S. A.*, 2004, **101**, 4781–4786.
97 G. Neuert, B. Munsky, R. Z. Tan, L. Teytelman, M. Khammash and A. van Oudenaarden, *Science*, 2013, **339**, 584–587.
98 J. Hasty, J. Pradines, M. Dolnik and J. J. Collins, *Proc. Natl. Acad. Sci. U. S. A.*, 2000, **97**, 2075–2080.
99 T. Tian and K. Burrage, *Proc. Natl. Acad. Sci. U. S. A.*, 2006, **103**, 8372–8377.
100 M. Hallen, B. Li, Y. Tanouchi, C. Tan, M. West and L. You, *PLoS Comput. Biol.*, 2011, **7**, e1002209.
101 P. C. Faucon, K. Pardee, R. M. Kumar, H. Li, Y.-H. Loh and X. Wang, *PLoS One*, 2014, **9**, e102873.
102 L.-Z. Wang, R.-Q. Su, Z.-G. Huang, X. Wang, W. Wang, C. Grebogi and Y.-C. Lai, 2015, arXiv150907038 Nlin Physicsphysics Q-Bio.
103 T. Tian and K. Burrage, *J. Chem. Phys.*, 2004, **121**, 10356–10364.
104 D. Bratsun, D. Volfson, L. S. Tsimring and J. Hasty, *Proc. Natl. Acad. Sci. U. S. A.*, 2005, **102**, 14593–14598.
105 A. T. Winfree, *J. Theor. Biol.*, 1967, **16**, 15–42.
106 M. Ishiura, S. Kutsuna, S. Aoki, H. Iwasaki, C. R. Andersson, A. Tanabe, S. S. Golden, C. H. Johnson and T. Kondo, *Science*, 1998, **281**, 1519–1523.
107 N. Barkai and S. Leibler, *Nature*, 2000, **403**, 267–268.
108 J. Tomita, M. Nakajima, T. Kondo and H. Iwasaki, *Science*, 2005, **307**, 251–254.
109 G. Buzsáki and A. Draguhn, *Science*, 2004, **304**, 1926–1929.
110 L. Ma, J. Wagner, J. J. Rice, W. Hu, A. J. Levine and G. A. Stolovitzky, *Proc. Natl. Acad. Sci. U. S. A.*, 2005, **102**, 14266–14271.
111 D. E. Nelson, A. E. C. Ihekwaba, M. Elliott, J. R. Johnson, C. A. Gibney, B. E. Foreman, G. Nelson, V. See, C. A. Horton, D. G. Spiller, S. W. Edwards, H. P. McDowell, J. F. Unitt, E. Sullivan, R. Grimley, N. Benson, D. Broomhead, D. B. Kell and M. R. H. White, *Science*, 2004, **306**, 704–708.
112 Q. Yang and J. E. Ferrell Jr, *Nat. Cell Biol.*, 2013, **15**, 519–525.
113 K. Pye and B. Chance, *Proc. Natl. Acad. Sci. U. S. A.*, 1966, **55**, 888–894.
114 B. Hess and A. Boiteux, *Annu. Rev. Biochem.*, 1971, **40**, 237–258.
115 L. F. Olsen and H. Degn, *Biochim. Biophys. Acta, Enzymol.*, 1978, **523**, 321–334.
116 J. Gerhart, M. Wu and M. Kirschner, *J. Cell Biol.*, 1984, **98**, 1247–1255.
117 J. C. Dunlap, *Cell*, 1999, **96**, 271–290.
118 J. Hasty, M. Dolnik, V. Rottschäfer and J. J. Collins, *Phys. Rev. Lett.*, 2002, **88**, 148101.
119 J. Stricker, S. Cookson, M. R. Bennett, W. H. Mather, L. S. Tsimring and J. Hasty, *Nature*, 2008, **456**, 516–519.
120 T. Y.-C. Tsai, Y. S. Choi, W. Ma, J. R. Pomerening, C. Tang and J. E. Ferrell, *Science*, 2008, **321**, 126–129.
121 M. Tigges, T. T. Marquez-Lago, J. Stelling and M. Fussenegger, *Nature*, 2009, **457**, 309–312.
122 F. K. Balagaddé, L. You, C. L. Hansen, F. H. Arnold and S. R. Quake, *Science*, 2005, **309**, 137–140.
123 F. K. Balagaddé, H. Song, J. Ozaki, C. H. Collins, M. Barnet, F. H. Arnold, S. R. Quake and L. You, *Mol. Syst. Biol.*, 2008, **4**, 187.
124 P. Marguet, Y. Tanouchi, E. Spitz, C. Smith and L. You, *PLoS One*, 2010, **5**, e11909.
125 T. Danino, O. Mondragón-Palomino, L. Tsimring and J. Hasty, *Nature*, 2010, **463**, 326–330.
126 B. Novák and J. J. Tyson, *Nat. Rev. Mol. Cell Biol.*, 2008, **9**, 981–991.
127 A. Prindle, P. Samayoa, I. Razinkov, T. Danino, L. S. Tsimring and J. Hasty, *Nature*, 2012, **481**, 39–44.
128 A. Prindle, J. Selimkhanov, H. Li, I. Razinkov, L. S. Tsimring and J. Hasty, *Nature*, 2014, **508**, 387–391.
129 Y. Chen, J. K. Kim, A. J. Hirning, K. Josić and M. R. Bennett, *Science*, 2015, **349**, 986–989.
130 K. Brenner, D. K. Karig, R. Weiss and F. H. Arnold, *Proc. Natl. Acad. Sci. U. S. A.*, 2007, **104**, 17300–17304.
131 T. A. Sanders, E. Llagostera and M. Barna, *Nature*, 2013, **497**, 628–632.
132 T. M. Jessell and E. R. Kandel, *Cell*, 1993, **72**, 1–30.
133 G. M. Dunny and B. A. B. Leonard, *Annu. Rev. Microbiol.*, 1997, **51**, 527–564.
134 A. J. Lee and L. You, *Science*, 2014, **343**, 624–625.
135 J. K. Srimani, G. Yao, J. Neu, Y. Tanouchi, T. J. Lee and L. You, *PLoS One*, 2014, **9**, e105408.
136 H. Youk and W. A. Lim, *Science*, 2014, **343**, 1242782.
137 M. S. Datta, K. S. Korolev, I. Cvijovic, C. Dudley and J. Gore, *Proc. Natl. Acad. Sci. U. S. A.*, 2013, **110**, 7354–7359.
138 R. Smith, C. Tan, J. K. Srimani, A. Pai, K. A. Riccione, H. Song and L. You, *Proc. Natl. Acad. Sci. U. S. A.*, 2014, **111**, 1969–1974.
139 H. Youk and W. A. Lim, *Science*, 2014, **343**, 1242782.
140 J. Garcia-Ojalvo, M. B. Elowitz and S. H. Strogatz, *Proc. Natl. Acad. Sci. U. S. A.*, 2004, **101**, 10955–10960.
141 C. C. Guet, M. B. Elowitz, W. Hsing and S. Leibler, *Science*, 2002, **296**, 1466–1470.
142 R. S. Cox, M. G. Surette and M. B. Elowitz, *Mol. Syst. Biol.*, 2007, **3**, 145.
143 S. Payne, B. Li, Y. Cao, D. Schaeffer, M. D. Ryser and L. You, *Mol. Syst. Biol.*, 2014, **9**, 697.
144 G. T. Reeves, C. B. Muratov, T. Schüpbach and S. Y. Shvartsman, *Dev. Cell*, 2006, **11**, 289–300.
145 S. Basu, Y. Gerchman, C. H. Collins, F. H. Arnold and R. Weiss, *Nature*, 2005, **434**, 1130–1134.
146 C. Liu, X. Fu, L. Liu, X. Ren, C. K. L. Chau, S. Li, L. Xiang, H. Zeng, G. Chen, L.-H. Tang, P. Lenz, X. Cui, W. Huang, T. Hwa and J.-D. Huang, *Science*, 2011, **334**, 238–241.
147 R. A. Fisher, *Ann. Eugen.*, 1937, **7**, 355–369.

148 D. E. Woodward, R. Tyson, M. R. Myerscough, J. D. Murray, E. O. Budrene and H. C. Berg, *Biophys. J.*, 1995, **68**, 2181–2189.
149 B. Momeni, A. J. Waite and W. Shou, *eLife*, 2013, **2**, e00960.
150 A. Kicheva, M. Cohen and J. Briscoe, *Science*, 2012, **338**, 210–212.
151 S. Strogatz, M. Friedman, A. J. Mallinckrodt and S. McKay, *Comput. Phys.*, 1994, **8**, 532.
152 C. Tan, H. Song, J. Niemi and L. You, *Mol. BioSyst.*, 2007, **3**, 343–353.
153 S. Kay, *Intuitive Probability and Random Processes using MATLAB®*, Springer Science & Business Media, 2006.
154 Y. A. Kuznetsov and S. Rinaldi, *Math. Biosci.*, 1996, **134**, 1–33.
155 J. Wang, *Adv. Phys.*, 2015, **64**, 1–137.
156 J. X. Zhou, M. D. S. Aliyu, E. Aurell and S. Huang, *J. R. Soc., Interface*, 2012, **9**, 3539–3553.
157 G. A. Huber and S. Kim, *Biophys. J.*, 1996, **70**, 97–110.
158 J. A. Kromer, L. Schimansky-Geier and R. Toral, *Phys. Rev. E: Stat., Nonlinear, Soft Matter Phys.*, 2013, **87**, 063311.

